

Study of defects in GaN grown by the two-flow metalorganic chemical vapor deposition technique using monoenergetic positron beams

A. Uedono,^{a)} S. F. Chichibu, and Z. Q. Chen^{b)}

Institute of Applied Physics, University of Tsukuba, Tsukuba, Ibaraki 305-8573, Japan

M. Sumiya

Department of Electrical and Electronic Engineering, Shizuoka University, 3-5-1 Johoku, Hamamatsu, Shizuoka 432-8561, Japan

R. Suzuki, T. Ohdaira, and T. Mikado

Electrotechnical Laboratory, 1-1-4 Umezono, Tsukuba, Ibaraki 305-8568, Japan

T. Mukai and S. Nakamura^{c)}

Nichia Chemical Industries Ltd., 491 Oka, Kaminaka, Anan, Tokushima 774-8601, Japan

(Received 4 January 2001; accepted for publication 22 March 2001)

Defects in GaN grown using metalorganic chemical vapor deposition were studied through the use of monoenergetic positron beams. For Mg-doped GaN, no large change in the diffusion length of positrons was observed before and after activation of Mg. This was attributed to the scattering of positrons by potentials caused by electric dipoles of Mg-hydrogen pairs. For Si-doped GaN, the line-shape parameter S increased as carrier density increased, suggesting an introduction of Ga vacancy due to the Fermi level effect. Based on these results, we discuss the effects of the growth polar direction of GaN on optical properties in this article. Although the optical properties of a GaN film grown toward the Ga face direction exhibited excitonic features, a film grown toward the N face ($-c$) direction exhibited broadened photoluminescence and transmittance spectra, and a Stokes shift of about 20 meV was observed. This difference was attributed to extended band-tail states introduced by high concentrations of donors and acceptor-type defects in $-c$ GaN. © 2001 American Institute of Physics. [DOI: 10.1063/1.1372163]

I. INTRODUCTION

Gallium nitride (GaN) and related alloys are the leading materials for the fabrication of optoelectronic devices such as light emitting diodes and laser diodes.¹ GaN films, for example, are usually fabricated on c -plane sapphire substrates using metalorganic chemical vapor deposition (MOCVD) or molecular beam epitaxy (MBE).²⁻⁵ Since GaN has a wurtzite structure having polarity along the c axis, two different surface structures exhibit the polarity of GaN; these are referred to as (0001) Ga face and (000 $\bar{1}$) N face. The polar surfaces of GaN have distinct effects on the growth processes and crystal quality of GaN layers.⁵⁻⁹ Although film polarity is one of the key parameters for the growth process of GaN, no clear correlation between defect-introduction mechanisms and film polarity has yet been established. The positron annihilation technique is an established means of studying defects in semiconductors.¹⁰ The implantation profile of monoenergetic positrons can be adjusted to a specific region of interest in the specimen by accelerating the positrons to a desired energy.¹¹ In general, the incident energy of monoenergetic positrons may vary from a few eV to 30–50 keV, and sampling can thus range from the surface of the specimen to a depth on the order of a few μm . Using this technique,

Saarinen and co-workers¹²⁻¹⁴ systematically studied native point defects in GaN films and in bulk crystal GaN. The characterization of GaN films grown on GaAs substrates and the formation mechanism of ohmic contacts of Pd on GaN have also been successfully studied with the use of a monoenergetic positron beam.^{15,16} These studies have shown that monoenergetic positrons can be a useful probe for studying vacancy-type defects in GaN. In the present work, monoenergetic positron beams were used to study the annihilation characteristics of positrons in very high-quality GaN films grown using two-flow MOCVD.³ From the results obtained, we characterized point defects in GaN layers grown along different polar directions.

When a positron is implanted into condensed matter, it annihilates with an electron mainly into two 511 keV γ quanta.¹⁰ The motion of the positron-electron pair causes a Doppler shift in the energy of the annihilation radiation. In a material containing defects, a freely diffusing positron may be localized in a vacancy-type defect because of the Coulomb repulsion from ion cores. Since the momentum distribution of electrons in such defects is different from that in the bulk, one can detect vacancy-type defects by measuring the Doppler broadening spectra of the annihilation radiation. The change in the Doppler broadening spectrum is characterized by the S parameter or the W parameter,^{10,11} S and W mainly characterize the fraction of the annihilation of positron-electron pairs with a low-momentum distribution and that of the annihilation of pairs with a high-momentum

^{a)}Electronic mail: uedono@ims.tsukuba.ac.jp

^{b)}On leave from Department of Physics, Wuhan University, Wuhan 430072, People's Republic of China.

^{c)}Present address: Department of Materials Engineering, University of California, Santa Barbara, CA 93106.

TABLE I. Carrier concentration n for the GaN films deposited on sapphire substrates by MOCVD.

Sample	n (cm ⁻³)
+ c GaN	5.0×10^{17}
- c GaN	3.5×10^{18}
Undoped GaN(LEO)	semi-insulating
Si-doped GaN (1)	1.6×10^{18}
Si-doped GaN (2)	1.9×10^{18}
Si-doped GaN (3)	2.2×10^{18}

distribution, respectively. The values of S and W differ depending on the specific type of defects; the S value, for example, increases with increasing size of the open volume of defects. When positrons are trapped by vacancy-type defects, their lifetime increases because of a reduced electron density in such defects. Measurements of the lifetime spectra of positrons provide useful information for identifying vacancy-type defects.

II. EXPERIMENT

In our experiments, we used undoped, Si-doped, and Mg-doped GaN/sapphire samples prepared by Nichia Chemical Industries Ltd. Undoped GaN crystal with reduced dislocation density was grown by the lateral epitaxial overgrowth (LEO) technique using the two-flow MOCVD method. After the growth, the substrate and SiO₂ mask patterns were removed to obtain a free-standing GaN layer with a thickness of about 70 μm . The resistivity of this sample was extremely high, indicating a small amount of residual impurities. Lattice constants were measured by the Bond method and found to be $a = 0.31898 \pm 0.00002$ nm and $c = 0.51855 \pm 0.00002$ nm. This shows that the sample is nearly free from residual strain. The optical properties of GaN grown using the same technique we used in our experiments have been reported elsewhere.¹⁷⁻¹⁹ Mg- and Si-doped GaN layers 1–3 μm thick were also grown on sapphire substrates using the two-flow MOCVD technique. After the Mg deposition, isochronal annealing was performed in an N₂ atmosphere in the temperature range between 100 and 1000 $^{\circ}\text{C}$ for 20 min in order to activate Mg;²⁰ the thickness of the Mg-doped region was about 0.5 μm . The carrier densities of Si-doped GaN are summarized in Table I. For Si-doped GaN, transmittance and photoluminescence (PL) spectra were measured at room temperature. PL was excited by the 325.0 nm line of a cw He–Cd laser (15 mW). A 300 W Xe lamp was used as a probe light for transmittance measurements. The transmitted light and PL were dispersed by a 67 cm focal-length grating monochromator (McPherson 207) and detected by a GaAs:Cs photomultiplier. The system has an accuracy of 0.3 meV and resolution of 0.5 meV at a wavelength of 350 nm.

Next, we characterized unintentionally doped 1- μm -thick GaN films. These films were deposited at 1040 $^{\circ}\text{C}$ using an atmospheric-pressure MOCVD system constructed in Shizuoka University. A detailed explanation of the deposition conditions is reported elsewhere.^{8,21} Optimized + c and - c GaN layers were obtained under different V/III ratios;

the Ga and N faces are referred to as having + c and - c polarity, respectively. The polar directions of the samples were determined by coaxial impact collision ion scattering spectroscopy.^{8,21} The surface morphology of + c GaN was smooth, but that of - c GaN was hexagonal facets. Using the van der Pauw method, we determined the sample's electron density n ; the results obtained are summarized in Table I. According to Sumiya *et al.*,²¹ the residual concentrations of carbon, oxygen, and Al in - c GaN are 1 or 2 orders of magnitude higher than those in + c GaN. Thus, the difference between the values of n for + c and - c GaN (Table I) is likely due to a difference in impurity concentration.

Doppler broadening spectra of the annihilation radiation were measured with a Ge detector as a function of the incident positron energy E . Spectra with a total count number of 5×10^5 were measured for each value of E and characterized by the S and W parameters; the central region of the spectra was defined as 511 ± 0.75 keV, and the wing region of the spectra was defined as from 511 ± 3.4 to 511 ± 6.7 keV. The relationship between the S parameter and E was analyzed using the computer program VEPFIT developed by van Veen *et al.*²² Details of the application of VEPFIT for the analysis of the S - E relationship are described elsewhere.^{22,23} The one-dimensional diffusion model of positrons is expressed by¹⁰

$$D_+ \frac{d^2}{dz^2} n(z) - \kappa_{\text{eff}}(z)n(z) + P(z, E) = 0, \quad (1)$$

where D_+ is the diffusion coefficient of positrons, $n(z)$ is the probability density of positrons at a distance z from the surface, $\kappa_{\text{eff}}(z)$ is the effective escape rate of positrons from the diffusion process, and $P(z, E)$ is the implantation profile of positrons. The diffusion length of positrons $L_d(z)$ is given by $L_d(z) = \sqrt{D_+ / \kappa_{\text{eff}}(z)}$. In the present work, the region sampled by positrons was divided into several blocks. Under this condition, VEPFIT solves Eq. (1). The observed S - E relationships were fitted to the relationship

$$S(E) = S_s F_s(E) + \sum S_i F_i(E), \quad (2)$$

where $F_s(E)$ is the fraction of positrons annihilated at the surface, $F_i(E)$ is that in the i th block [$F_s(E) + \sum F_i(E) = 1$], and S_s and S_i are the S parameters for the annihilation of positrons at the surface and in the i th block, respectively. The effect of the annihilation of epithermal positrons on the S - E curves was also included in the fitting procedure.¹¹

Lifetime spectra of positrons were measured with a pulsed monoenergetic positron beam.²⁴ For each lifetime spectrum, about 1×10^6 counts were accumulated and E was fixed at 10 keV during the measurements. The observed spectra were analyzed using the computer program RESOLUTION²⁵ with a time resolution (full width at half maximum) of about 290 ps.

III. RESULTS AND DISCUSSION

A. Annihilation characteristics of positrons in undoped, Mg-doped, and Si-doped GaN

Figure 1 shows the S parameter as a function of E for some GaN samples grown by MOCVD. The mean implantation depth of positrons is given on the upper axis. This

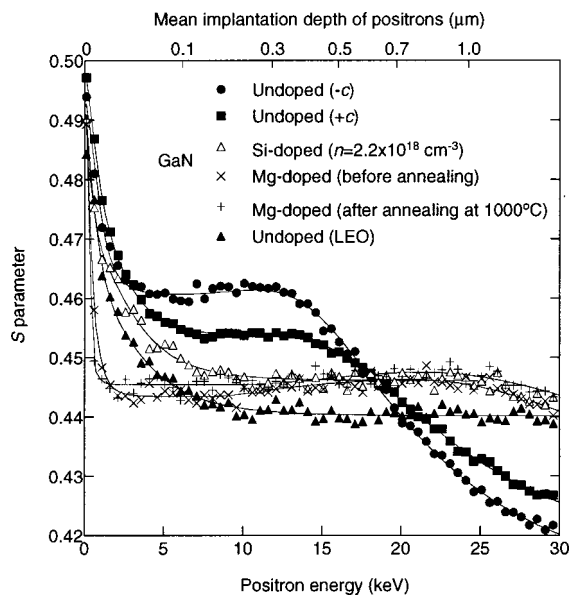


FIG. 1. S parameter as a function of incident positron energy for undoped, Mg-doped, and Si-doped GaN fabricated by MOCVD. The solid curves are the results of the fitting, and the derived parameters for Mg-doped GaN are shown in Fig. 2.

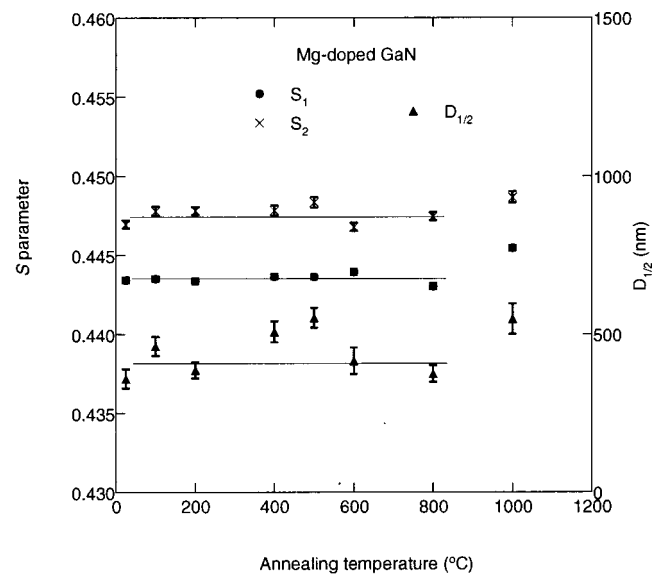


FIG. 2. Annealing behaviors of the characteristic values of S corresponding to the annihilation of positrons in the first and second blocks (S_1 and S_2) and the position of the interface between those blocks ($D_{1/2}$) for Mg-doped GaN. The first and second blocks correspond to the Mg-doped and undoped GaN regions, respectively.

section mainly discusses the annihilation characteristics of positrons in undoped, Mg-doped, and Si-doped GaN. For undoped GaN, S approaches a constant value at high E (>10 keV), which indicates that in this energy range almost all positrons annihilate in the bulk without diffusing back to the surface. The increase in S at low E ($\cong 0$ keV) is due to the annihilation of positrons and positronium atoms at the surface.²⁶ For undoped GaN, the S - E curve was fitted to Eq. (2); the distribution of S was assumed to be homogeneous. The solid curve shown in Fig. 1 is the fitting result. The diffusion length of positrons L_d and the value of S for the annihilation of positrons in the bulk S_b were determined to be 51 ± 2 nm and 0.4401 ± 0.0001 , respectively. The derived value of L_d for undoped GaN is the longest ever reported. From measurements of time-resolved PL spectra for undoped GaN grown by LEO, the first and second decay of the signal were determined to be 130 and 860 ps, respectively.¹⁷ The second lifetime shows that the crystal quality of undoped GaN is very high. Thus, the derived long diffusion length of positrons in undoped GaN can be linked to the high quality of the sample. However, the typical value of L_d in semiconductors such as Si,^{27,28} Ge,²⁹ and GaAs (Ref. 30), is 200–300 nm, and that in metals such as Ni^{31,32} and Cu (Ref. 33) is 150–200 nm. Since the value of L_d for undoped GaN is shorter than the typical value of L_d in defect-free materials, the diffusion of positrons in undoped GaN is likely to be suppressed by the trapping or scattering of defects. As discussed below, the positrons in GaN are likely to be scattered by electrically inactive or compensated impurities; this process does not affect the value of S . Since the value of S_b for undoped GaN is the lowest S_b value we obtained in our experiments, we consider it to be close to the characteristic value of S for the annihilation of positrons from the free state.

The S - E curves for Mg-doped GaN before and after annealing were fitted to Eq. (2). In the fitting procedure, the region sampled by positrons was divided into three blocks; the third block corresponds to the sapphire substrate. Respective S_b and L_d values of 0.4109 ± 0.0001 and 46.7 ± 0.4 nm were obtained from the S - E curve for the sapphire substrate. Figure 2 shows annealing behaviors of the characteristic values of S corresponding to the annihilation of positrons in the first and second blocks (S_1 and S_2) and the position of the interface between those blocks ($D_{1/2}$). Since the width of the first block just coincides with that of the Mg-doped region, the first and second blocks correspond to the Mg-doped and undoped GaN regions, respectively. In the S - E curves for Mg-doped GaN before annealing and after annealing at 1000 °C (Fig. 1), the sharp decrease in S just below the surface ($E < 1$ keV) is due to the effects of the epilayer positrons and/or the short diffusion length of positrons on S . The former, however, was not considered in the fitting procedure. The diffusion length of positrons in the first block L_{d1} for the sample before and after annealing was almost constant (about 1 nm); the diffusion length of positrons in the second block L_{d2} was assumed to be the same as that of L_{d1} . Nakamura *et al.*²⁰ reported that Mg can be activated by thermal annealing above 700 °C. Thus, one can conclude that, before and after activation of Mg, almost all positrons are trapped by defects and cannot escape from the surface.

In boron- or As-doped Si, for example, activated impurities suppress the diffusion of positrons because positrons are trapped or scattered by such charged impurities, or it also could be suppressed by the electric field in the subsurface region.^{33,34} In GaN, as mentioned above, the diffusion of positrons is likely to be suppressed by Mg before activation. It has been suggested that hydrogen coming from MOCVD precursors neutralizes Mg; the sites of hydrogen are in anti-

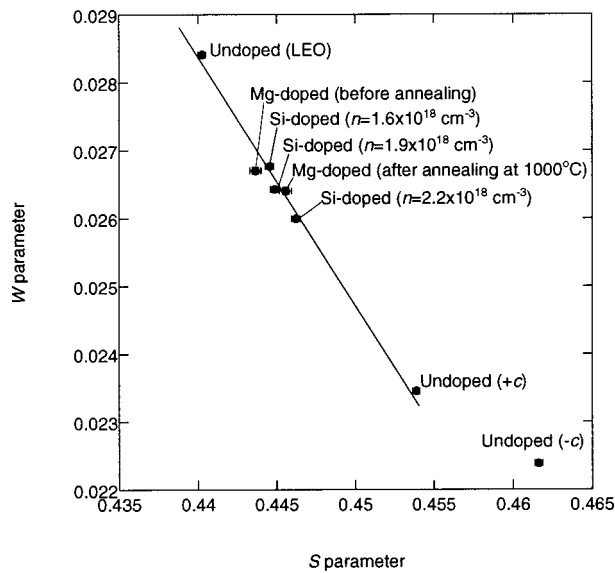


FIG. 3. The S - W relationships for undoped, Mg-doped, and Si-doped GaN films deposited on sapphire substrates by MOCVD. The solid lines are intended to serve as a guide to the eye.

bonding position^{35,36} or in bond center (BC)³⁷ location. In Mg-doped GaN before activation, positrons might be scattered by potentials caused by electric dipoles of Mg-H complexes. Since the potential introduced by the dipoles increases as the distance between Mg and hydrogen increases, Mg-H complexes at the BC location are likely to suppress the diffusion of positrons effectively. From Fig. 2, it can be seen that no large change in the value of S_1 was observed below 800 °C, and the value of S in the undoped region (S_2) is larger than that of S_1 ; the S_1 value is the lowest one we obtained except for that of undoped GaN (LEO). Thus, in Mg-doped GaN, the scattering of positrons by Mg-H complexes is considered to suppress the trapping of positrons by defects. After annealing at 1000 °C (Figs. 1–3), the value of S corresponding to the Mg-doped region increases, suggesting the trapping of positrons by vacancy-type defects. Nakamura and Fasol³⁸ reported that a decrease in intensity of blue emission starts above annealing at 500 °C, suggesting the dissociation of GaN. This phenomenon may thus be related to the introduction of vacancy-type defects observed in our experiments.

For Si-doped GaN, the S - E curves were fitted to Eq. (2); the distribution of S was assumed to be homogeneous. The value of L_d obtained for all Si-doped GaN samples was about 35 nm. This value is shorter than the L_d value for undoped GaN (LEO), suggesting the trapping of positrons by defects. To increase the statistical accuracy of Doppler broadening spectra corresponding to the annihilation of positrons in Si-doped GaN, we integrated the spectra measured at $E = 10$ –25 keV into one spectrum, and the values of S and W were calculated using this spectrum. Figure 3 shows the relationship between S and W for Si-doped GaN; the S values for Si-doped GaN are larger than that for undoped GaN (LEO). We used a limited number of Si-doped samples in our experiments, but the value of S appears to increase as the carrier density increases. The formation energies for native

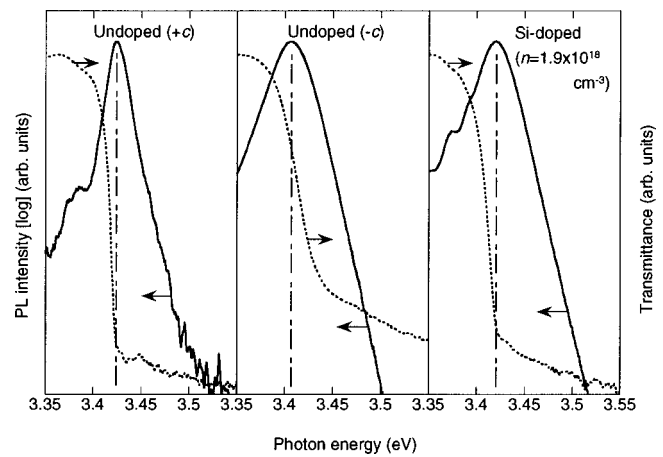


FIG. 4. Comparison of photoluminescence and transmittance spectra for $+c$, $-c$, and Si-doped GaN ($n = 1.9 \times 10^{18} \text{ cm}^{-3}$). The Stokes shift of about 20 meV was observed for $-c$ GaN. This was attributed to extended band-tail states introduced by high concentrations of donors and acceptor-type defects.

point defects in GaN were obtained using first-principles calculation.^{39,40} According to the calculation results, a Ga vacancy (V_{Ga}) is an acceptor-type defect, hence its formation energy decreases as the Fermi level increases. According to Saarinen and co-workers,^{12–14} V_{Ga} is the major point defect that can be detected by positrons. Thus, the observed increase in S for Si-doped GaN might be attributed to an increase in V_{Ga} concentration due to the Fermi level effect.

B. Vacancy-type defects in $+c$ and $-c$ GaN

Figure 4 shows transmittance and PL spectra for $+c$, $-c$, and Si-doped GaN ($n = 1.9 \times 10^{18} \text{ cm}^{-3}$). Details of optical absorption and PL spectra for $+c$ and $-c$ GaN are reported elsewhere.⁴¹ The dominant characteristic of the PL spectrum for $+c$ GaN is the near-band-edge emission peak. Since the carrier density of $+c$ GaN is smaller than that required for Coulomb screening,^{41,42} the observed peak can be attributed to free exciton emission. The spectra for the Si-doped sample ($n = 1.9 \times 10^{18} \text{ cm}^{-3}$) are similar to those for $+c$ GaN. The observed optical properties of $+c$ GaN and Si-doped GaN are typical ones for high-quality GaN. Conversely, $-c$ GaN exhibits a rather broad PL band and a long tail in the transmittance spectrum. A Stokes shift of about 20 meV was observed for $-c$ GaN, although Si-doped GaN, which has similar electron density, did not show any Stokes shift. Thus, an impurity-induced band tail is likely to be formed in $-c$ GaN, which subsequently causes band gap narrowing.⁴¹

Figure 1 shows the S - E curves for $+c$ and $-c$ GaN; the curve shoulders at $E = 5$ –10 keV correspond to the annihilation of positrons in the GaN films. The S - E curves were fitted to Eq. (2), and the values of L_d obtained for $+c$ and $-c$ GaN were 23 ± 1 and 4.8 ± 0.2 nm, respectively. The value of S for $+c$ GaN is larger than that of $-c$ GaN. Thus, one can conclude that the size and/or the concentration of vacancy-type defects in $-c$ GaN are larger or higher than those in $+c$ GaN. The lifetime spectra of positrons with $E = 10$ keV for $+c$ and $-c$ GaN were decomposed into two

TABLE II. The lifetimes of positrons and their intensities for $+c$ and $-c$ GaN. The lifetime spectra of positrons with $E=10.0$ keV were measured using the pulsed monoenergetic positron beam, and decomposed into two components; τ_1 and I_i are the lifetime of the i th component and its intensity ($i=1$ and 2 ; $I_1+I_2=1$).

Sample	τ_1 (ps)	τ_2 (ps)	I_2 (%)
$+c$ GaN	189 ± 2	460 ± 10	11 ± 1
$-c$ GaN	203 ± 2	640 ± 10	7 ± 1

components. The obtained lifetimes of positrons and their intensities are summarized in Table II. Puska *et al.*⁴³ calculated the lifetimes of positrons trapped by V_{Ga} and by a divacancy to be 273 and 348 ps, respectively. Later, from measurements of lifetime spectra of positrons for bulk GaN, Saarinen *et al.*¹² determined that the lifetime of positrons trapped by V_{Ga} is 235 ps. Thus, in Table II, the second components for $+c$ and $-c$ GaN can be attributed to the annihilation of positrons trapped by open spaces which are larger than divacancies. Figure 3 shows the values of (S, W) for $+c$ and $-c$ GaN; these values were calculated from Doppler broadening spectra at $E=7-13$ keV. Although the carrier densities of $+c$ and $-c$ GaN are lower than or close to those for Si-doped GaN, the value of S is higher than that for Si-doped GaN. This suggests that vacancy-type defects in $+c$ and $-c$ GaN were not introduced by the Fermi level effect, but the annihilation mode of positrons trapped by the open spaces (the second component in Table II) is likely to contribute to the increase in S (or the decrease in W). Since the lifetimes of the first component are longer than those of positrons annihilated from the free state ($\tau_f=166$ ps), the annihilation mode of positrons trapped by point defects is likely to be incorporated into the first component.

In Fig. 3, the value of (S, W) for $+c$ GaN appears to intersect an extrapolated line which connects the values of (S, W) for undoped, Mg-doped, and Si-doped GaN. From the discussion in Sec. III A, this line is associated with the annihilation of positrons trapped by vacancy-type defects such as V_{Ga} . For $-c$ GaN, the value of (S, W) is located at the upper half of the figure, suggesting suppression of the decrease in the annihilation probability of positrons with electrons with a broadened momentum distribution. For Si, the characteristic value of S for vacancy-oxygen complexes is known to be smaller than that for "pure" vacancy-type defects.⁴⁴⁻⁴⁶ The decrease in S is due to the annihilation of positrons with electrons having a broadened momentum distribution, and this annihilation mode is introduced by the coupling of oxygen atoms with vacancy-type defects. Sumiya *et al.*²¹ reported that residual oxygen concentration in $-c$ GaN was 2 orders of magnitude higher than those in $+c$ GaN. Thus, the origin of the suppression of the decrease in W may be the annihilation of positrons trapped by vacancy-oxygen complexes. We have not yet clarified the relationship between the vacancy-oxygen complexes and the extended band tail in $-c$ GaN. But the difference between the S values and the lifetimes for $+c$ and $-c$ GaN clearly shows that the concentration of vacancy-type defects and their sizes in $-c$ GaN are higher than those in $+c$ GaN. Since acceptor vacancy-type defects trap positrons effectively, one possible explana-

tion for the formation of the band tail observed in transmittance and PL spectra is a narrowing of the band gap due to potential fluctuation in connection with an incorporation of acceptor-type defects and inhomogeneous distribution of fixed charges.

IV. CONCLUSIONS

We used monoenergetic positron beams to study defects in GaN films deposited on sapphire substrates by MOCVD. Doppler broadening spectra of the annihilation radiation and lifetime spectra of positrons were measured for undoped, Mg-doped, and Si-doped GaN samples. Based on those measurements, we characterized GaN films grown along different polar directions. We derived an L_d value of 51 ± 2 nm from measurements of the $S-E$ curve for a very high-quality GaN sample (undoped and free-standing) grown using LEO. This is the longest L_d value for GaN yet reported. However, since typical defect-free materials exhibit an L_d value of about 150–200 nm, it is clear that positrons are scattered or trapped by defects even in this high-quality sample. For Mg-doped GaN, no large change in the values of L_d was observed either before or after activation of Mg (≤ 800 °C). This was attributed to the scattering of positrons by potentials caused by electric dipoles of Mg-H pairs. For the three Si-doped GaN samples we characterized in our experiments, the value of S increased as carrier density increased. The formation energy of V_{Ga} is known to decrease as the Fermi level increases, due to the Fermi level effect. Thus, the observed increase in S may be due to the introduction of vacancy-type defects such as V_{Ga} .

On the basis of the above results, we discussed the effects of the growth polar direction of GaN on optical properties. Although $+c$ GaN exhibited clear excitonic features in optical properties, $-c$ GaN exhibited a broadened photoluminescence and transmittance spectra; a Stokes shift of about 20 meV was observed. The difference between optical properties of $+c$ and $-c$ GaN was attributed to extended band-tail states introduced by high concentrations of donors and acceptor-type defects in $-c$ GaN. Our results demonstrate that the monoenergetic positron beam technique can be a useful tool for the study of vacancy-type defects in GaN films grown by MOCVD.

ACKNOWLEDGMENTS

The authors would like to thank A. Setoguchi, M. Sugiyama, K. Yoshimura, M. Muramatsu, and T. Ubukata for their assistance with the preparation and characterization of the samples.

¹S. P. DenBaars, *Introduction to Nitride Semiconductor, Blue Lasers and Light Emitting Diodes*, edited by S. Nakamura and S. F. Chichibu (Taylor & Francis, London, 2000), p. 1.

²H. Amano, M. Kito, K. Hiramatsu, and I. Akasaki, *Jpn. J. Appl. Phys.*, Part 2 **28**, L2112 (1989).

³S. Nakamura, *Jpn. J. Appl. Phys.*, Part 2 **30**, L1705 (1991).

⁴T. Lei, M. Fanciulli, R. J. Molnar, T. D. Moustakas, R. J. Graham, and J. D. Scanlon, *Appl. Phys. Lett.* **59**, 944 (1991).

⁵F. A. Ponce, D. P. Bour, W. T. Young, M. Saunders, and J. W. Steeds, *Appl. Phys. Lett.* **69**, 337 (1996).

⁶S. Keller, B. P. Keller, Y.-F. Wu, B. Heying, D. Kapolnek, J. S. Speck, U.

- K. Mishra, and S. P. Denbaars, *Appl. Phys. Lett.* **68**, 1525 (1996).
- ⁷J. L. Rouviere, J. L. Weyher, M. Seelmann-Eggebert, and S. Porowski, *Appl. Phys. Lett.* **73**, 668 (1998).
- ⁸M. Sumiya, M. Tanaka, K. Ohtsuka, S. Fuke, T. Ohnishi, I. Ohkubo, M. Yoshimoto, H. Koinuma, and M. Kawasaki, *Appl. Phys. Lett.* **75**, 674 (1999).
- ⁹F. Bernardini and V. Fiorentini, *Phys. Rev. B* **57**, R9427 (1998); *Phys. Status Solidi B* **216**, 391 (1999).
- ¹⁰R. Krause-Rehberg and H. S. Leipner, *Positron Annihilation in Semiconductors*, Solid-State Sciences, Vol. 127 (Springer, Berlin, 1999).
- ¹¹P. G. Coleman, *Positron Beams and Their Application* (World Scientific, Singapore, 2000), p. 1.
- ¹²K. Saarinen *et al.*, *Phys. Rev. Lett.* **79**, 3030 (1997).
- ¹³K. Saarinen, P. Seppälä, J. Oila, P. Hautojärvi, C. Corbel, O. Briot, and R. L. Aulombard, *Appl. Phys. Lett.* **73**, 3253 (1998).
- ¹⁴K. Saarinen, J. Nissilä, P. Hautojärvi, J. Likonen, T. Suski, I. Grzegory, B. Lucznik, and S. Porowski, *Appl. Phys. Lett.* **75**, 2441 (1999).
- ¹⁵P. Rice Evans, A. S. Saleh, M. Nathwani, J. W. Taylor, and C. T. Foxon, *Appl. Surf. Sci.* **149**, 165 (1999).
- ¹⁶J.-L. Lee, M. Weber, J. K. Kim, J. W. Lee, Y. J. Park, T. Kim, and K. Lynn, *Appl. Phys. Lett.* **74**, 2289 (1999).
- ¹⁷S. F. Chichibu *et al.*, *Appl. Phys. Lett.* **74**, 1460 (1999).
- ¹⁸K. Torii, T. Deguchi, T. Sota, K. Suzuki, S. Chichibu, and S. Nakamura, *Phys. Rev. B* **60**, 4723 (1999).
- ¹⁹S. F. Chichibu, K. Torii, T. Deguchi, T. Sota, A. Setoguchi, H. Nakanishi, T. Azuhata, and S. Nakamura, *Appl. Phys. Lett.* **76**, 1576 (2000).
- ²⁰S. Nakamura, T. Mukai, M. Senoh, and N. Iwasa, *Jpn. J. Appl. Phys., Part 2* **31**, L139 (1992).
- ²¹M. Sumiya, K. Yoshimura, K. Ohtsuka, and S. Fuke, *Appl. Phys. Lett.* **76**, 2098 (2000).
- ²²A. van Veen, H. Schut, M. Clement, J. M. M. de Nijs, A. Kruseman, and M. R. Ijpma, *Appl. Surf. Sci.* **85**, 216 (1995).
- ²³A. Uedono *et al.*, *J. Appl. Phys.* **87**, 4119 (2000).
- ²⁴R. Suzuki, Y. Kobayashi, T. Mikado, H. Ohgaki, M. Chiwaki, T. Yamazaki, and T. Tomimasu, *Jpn. J. Appl. Phys., Part 2* **30**, L532 (1991).
- ²⁵P. Kirkegaard, M. Eldrup, O. E. Mogensen, and N. J. Pedersen, *Comput. Phys. Commun.* **23**, 307 (1981).
- ²⁶R. Suzuki *et al.*, *Jpn. J. Appl. Phys., Part 1* **37**, 4636 (1998).
- ²⁷B. Nielsen, K. G. Lynn, D. O. Welch, T. C. Leung, and G. W. Rubloff, *Phys. Rev. B* **40**, 1434 (1989).
- ²⁸A. Uedono, M. Watanabe, S. Takasu, T. Sabato, and S. Tanigawa, *J. Phys.: Condens. Matter* **12**, 719 (2000).
- ²⁹A. Uedono, T. Moriya, N. Komuro, T. Kawano, S. Tanigawa, and A. Ikari, *Jpn. J. Appl. Phys., Part 1* **35**, 4599 (1996).
- ³⁰A. Uedono, L. Wei, Y. Tabuki, H. Kondo, S. Tanigawa, K. Wada, and H. Nakanishi, *Jpn. J. Appl. Phys., Part 2* **30**, L2002 (1991).
- ³¹K. G. Lynn, D. M. Chen, B. Nielsen, R. Pareja, and S. Myers, *Phys. Rev. B* **34**, 1449 (1986).
- ³²A. Uedono, S. Tanigawa, and H. Sakairi, *J. Nucl. Mater.* **184**, 191 (1991).
- ³³A. Uedono, T. Kitano, K. Hamada, T. Moriya, T. Kawano, S. Tanigawa, R. Suzuki, T. Ohdaira, and T. Mikado, *Jpn. J. Appl. Phys., Part 1* **36**, 2571 (1997).
- ³⁴A. Uedono *et al.*, *Jpn. J. Appl. Phys.* (accepted for publication).
- ³⁵J. Neugebauer and C. G. Van de Walle, *Phys. Rev. Lett.* **75**, 4452 (1995).
- ³⁶B. Clerjaud, D. Cote, A. Lebkiri, C. Naud, J. M. Baranowski, K. Pakula, D. Wasik, and T. Suski, *Phys. Rev. B* **61**, 8238 (2000).
- ³⁷Y. Okamoto, M. Saito, and A. Oshiyama, *Jpn. J. Appl. Phys., Part 2* **35**, L807 (1996).
- ³⁸S. Nakamura and G. Fasol, *The Blue Laser Diode* (Springer, Berlin, 1997).
- ³⁹J. Neugebauer and C. G. Van de Walle, *Phys. Rev. B* **50**, 8067 (1994).
- ⁴⁰P. Boguslawski, E. L. Briggs, and J. Bernholc, *Phys. Rev. B* **51**, 17255 (1995).
- ⁴¹S. F. Chichibu, A. Setoguchi, A. Uedono, K. Yoshimura, and M. Sumiya, *Appl. Phys. Lett.* **78**, 28 (2001).
- ⁴²S. Chichibu, T. Azuhata, T. Sota, and S. Nakamura, *J. Appl. Phys.* **79**, 2784 (1996); S. Chichibu, K. Torii, T. Deguchi, T. Sota, A. Setoguchi, H. Nakanishi, T. Azuhata, and S. Nakamura, *Appl. Phys. Lett.* **76**, 1576 (2000).
- ⁴³M. J. Puska, S. Mäkinen, M. Manninen, and R. M. Nieminen, *Phys. Rev. B* **39**, 7666 (1989).
- ⁴⁴B. Nielsen, K. G. Lynn, T. C. Leung, B. F. Cordts, and S. Seraphin, *Phys. Rev. B* **44**, 1812 (1991).
- ⁴⁵A. Uedono, Y. Ujihira, A. Ikari, H. Haga, and O. Yoda, *Hyperfine Interact.* **79**, 615 (1993).
- ⁴⁶S. Eichler, J. Gebauer, F. Borner, A. Polity, R. Krauserehberg, E. Wendler, B. Weber, W. Wesch, and H. Borner, *Phys. Rev. B* **56**, 1393 (1997).